Supporting Information

Electrochemiluminescence Induced Photoelectrochemical for Sensing of the DNA Based on DNA-Linked CdS NPs Superstructure with intercalator molecules

Yingshu Guo, Yuanshun Sun, Shusheng Zhang*

State Key Laboratory Base of Eco-chemical Engineering; College of Chemistry and Molecular Engineering, Qingdao University of Science and Technology, Qingdao 266042, China

* Corresponding author. Tel.: +86-532-84022750; Fax: +86-532-84022750.

E-mail: shushzhang@126.com

Materials. DNA was synthesized by SBS Genetech Inc. Sequences of the oligonucleotides are listed in Table 1. 1-ethyl-3-(3-dimethylaminopropyl)-carbodiimide hydrochloride (EDC) was purchased from Sigma. Mercaptoethylamine (MCH) was obtained from Fluka (USA). All of the other reagents were purchased from Sinopharm Chemical Reagent Co. Ltd. and used without further purification. Phosphate buffer solutions (0.1 mol/L) with various pH values were prepared by mixing stock standard solutions of K_2HPO_4 and KH_2PO_4 and adjusting the pH with 0.1 mol/L H_3PO_4 or NaOH. Deionized and doubly distilled water was used throughout all of the experiments.

Table S1. ssDNA Sequences

DNA	Sequences (5′to 3′)	Description
S1	5'-SH-$(CH_2)_6$-TCG TAC GAT CGA TCC-3'	thiolated probe immobilized on Au electrode
S2	5'-GCC GCT CAC ACG ATA TTT TTT GGA TCG ATC GTA CGA-3'	target DNA complementary to S1 and S3
S3	5'-TAT CGT GTG AGC GGC TTT TTT-$(CH_2)_6$-NH_2-3'	amino probe functionalized on CdS NPs and complementary S2
S4	5'-GCT CAT ATG GAC CTC TTT TTT-$(CH_2)_6$-NH_2-3'	amino probe functionalized on CdS NPs and complementary S5
S5	5'-GAG GTC CAT ATG AGC TTT TTT-$(CH_2)_6$-NH_2-3'	amino probe functionalized on CdS NPs and complementary S4
S6	5'-GCC GCT CAC ACG ATA TTT TTT GGA TCG GTC GTA CGA-3'	the underlined base was the mismatched base
S7	5'-ACA TGC TTG GAC TGC TTT TTT CAG GCT CAT CGT ACG-3'	noncomplementary ssDNA

Apparatus. ECL singals were achieved by a MPI-A ECL analyzer (Xi'An Remax Electronic Science & Technology, Xi'An, China) using a three-electrode system. An Au electrode (diameter 4 mm) acted as a working electrode. A Pt wire acted as a counter electrode. An Ag/AgCl electrode acted as a reference electrode. Photocurrent and electrochemical impedance spectroscopy (EIS) were recorded by a CHI 660C electrochemical workstation (Shanghai CH Instruments, China). Scanning electron microscopy (SEM) images was obtained using a JEOL JSM-6340 F instrument

(Hitachi, Japan). UV-vis adsorption spectrum was carried out on a Cary 50 UV–Vis–NIR spectrophotometer (Varian). Photocurrent spectrum was obtained by MPI-EO photochemistry analyzer (Xi'An Remax Electronic Science & Technology, Xi'An, China). The ECL spectra were measured on a model FL 4500 spectrofluorometer (HITACHI)-ECL analyzer.

Synthesis of CdS nanoparticles (CdS NPs). Carboxyl modified CdS NPs were prepared according to the literature [1] with a slight modification. In brief, 0.0161 g of $CdC1_2 \cdot 2.5\ H_2O$ was dissolved in 50.0 mL water and 4.0 μL mercaptoacetic acid was added under stirring. The pH was then adjusted to 11 using 0.5 M NaOH under stirring and N_2 bubbling. Then 50 mL of 1.34 mM Na_2S solution was slowly added dropwise. After refluxing for 24 h under N_2 bubbling, CdS NPs was obtained and stored at 4°C. Fig. S1 shows the SEM image of CdS NPs.

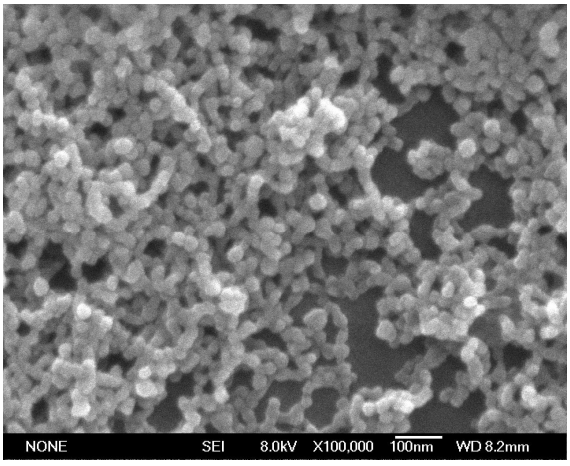

Fig. S1 SEM image of CdS NPs.

Preparation of ssDNA-functionalized CdS NPs. Three kinds of functionalized CdS NPs was synthesized. One is bio barcode-functionalized CdS NPs. A mixture of 1.0×10^{-10} mol of S3 and 1.0×10^{-9} mol of S4 was added to the CdS NPs in 500 μL of phosphate buffer (0.1 M, pH 7.4) that included 10 mM EDC, and incubated at 37 ºC for 2 h. The resulting bio barcode functionalized CdS NPs were centrifuged to remove excess ssDNA. One is S 4- functionalized CdS NPs. 500 μL of CdS NPs included 10 mM EDC were incubated with 1.0×10^{-7} M of S 4 at 37 ºC for 2 h. The

resulting S4-functionalized CdS NPs were centrifuged to remove excess S4. For the preparation of S5-functionalized CdS NPs, the same procedure as described for the preparation of S4-functionalized CdS NPs was followed. The functionalized CdS NPs were all stored in 200 μL of phosphate buffer (0.1 M, pH 7.4) at 4 ºC, respectively.

Fabrication of the work electrodes

Au electrode 1 was polished with 1.0, 0.3, 0.05 μm α-Al_2O_3 powder. After washed ultrasonically with deionized and doubly distilled water, the electrode was dried with nitrogen gas to remove any remaining impurities. The prepared Au electrode 1 was used as work electrode for Luminol ECL.

The pretreatment of Au electrode 2 was the same procedure as described for the preparation of Au electrode 1. After drying with nitrogen, Au electrode 2 was immersed in 1.0 mL of 0.1 phosphate buffer containing 1.0×10^{-7} M thiolated S1 at room temperature overnight. The electrode was then washed with water and immersed in 1.0 mM MCH for 1 h to prevent nonspecific absorption of DNA on the electrode surface. For the hybridization step, S1-modified electrode was incubated with target DNA solutions in 0.1 M phosphate buffer for 1 h at 37 ºC. Subsequent interaction of the electrode with a mixture containing 200 μL of bio barcode-functionalized CdS NPs, 200 μL of S5-functionalized CdS NPs, 200 μL of S4-functionalized CdS NPs and 5.0×10^{-5} M MB at 37 ºC resulted in the binding of the DNA-linked CdS NPs superstructure with MB to the electrode surface. The hybridization procedure resulted in the fabrication of a sandwich-type protocol. Then the electrode was rinsed with 0.1 M phosphate buffer to remove nonspecifically adsorbed residues. Electrochemical impedance spectroscopy (EIS) can give information on the impedance changes of the electrode surface in the modification

process. Furthermore, the fabrication process of the biosensor was characterized by EIS as shown in Fig. S2. An almost straight line was exhibited, which was characteristic of a mass diffusional limiting electron-transfer process (Fig. S2 a). After the electrode was treated with S1 and MCH, the EIS showed a small interfacial *eT* resistance (Fig. S2 b). Subsequently, target DNA was hybridized with S1 and *R*et increased (Fig. S2 c). After assembly DNA-linked CdS NPs superstructure on the electrode, the interfacial resistance (Fig. S2 d) remarkably increased. These results matched the fact that the electrode was fabricated as expectation.

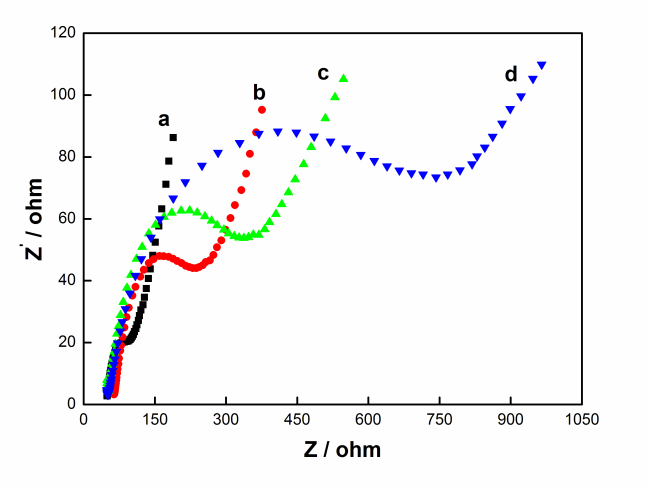

Fig. S2 EIS of (a) the bare Au electrode, (b) S1 and MCH modified Au electrode 2(c) target DNA hybridized with S1 assembled on the surface of the Au electrode 2 and (d) the Au electrode 2 of the other end of the targre DNA is recognized by DNA-linked CdS NPs superstructure.

Optimum of the pH value and concentration of Luminol solution

The ECL intensity of Luminol was related to photocurrent. The ECL efficiencies were strongly influenced by various factors, such as the pH value and Luminol concentration. So effect of the pH value and Luminol concentration were studied. The effect of Luminol solution in the pH range from 7.0 to 13.0 was investigated (Fig. S3A). When the pH was lower than pH 12.0, the ECL intensity increased with increasing pH; when the pH of Luminol solution was higher than pH 12.0,

the ECL intensity would go down with increasing pH. The optimized pH condition for Luminol ECL was pH 12.0. Luminol concentrations over the range from 1.0×10^{-4} to 2.0×10^{-2} M at pH 12.0 were examined (Fig. S3B). It was found that the intensity of all ECL intensities increased significantly with an increase in Luminol concentration, which was agreed with literature. [2]

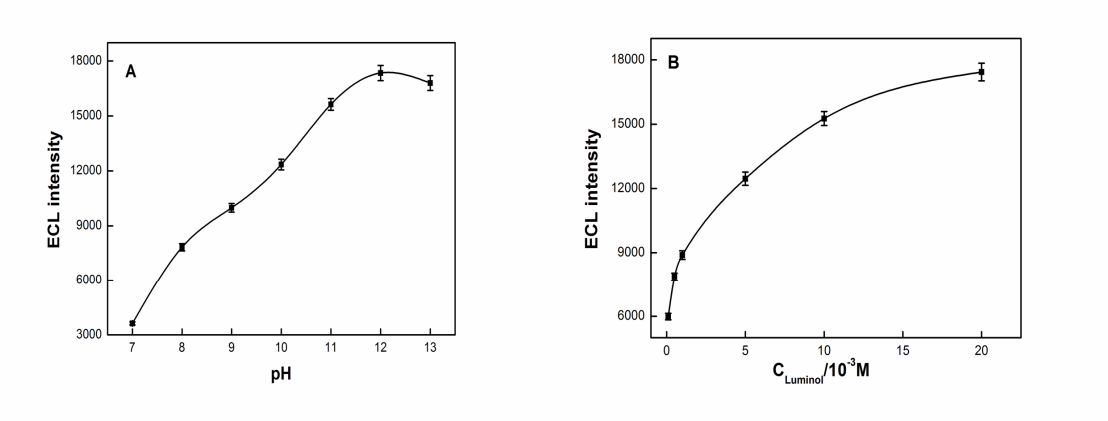

Fig. S3 The influence of (A) pH value and (B) Luminol concentration on ECL intensities

Optimum of the assembly DNA-linked CdS NPs superstructure time

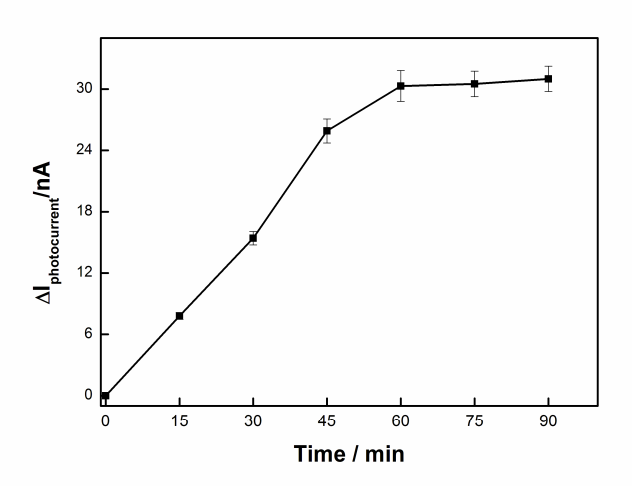

Fig. S4 The influence of the assembly DNA-linked CdS NPs superstructure time on photocurrent. The concentration of target DNA was 1.0×10^{-14} M.

The performance of the strategy mainly depended on the amounts of CdS NPs in DNA-linked CdS NPs superstructure. The effect of the assembly time was examined over the range of 15-90 min using 1.0×10^{-14} M DNA solution. As shown in Fig. S4, the photocurrent increased with

increasing assembly time and reached a maximum value at 60 min. At times longer than 60 min, the increase was no longer significant. On the basis of these results, an incubation time of 60 min was chosen for all further experiments.

A UV-vis spectrum of CdS NPs is shown in Fig. S5 A. A photocurrent spectrum of the proposed method is displayed in Fig. S5 B. The UV-vis spectrum was similar to the photocurrent spectrum. And it revealed that the photoactivity was due to the CdS NPs. Based on Fig. S5 B and Fig. S5 C, a conclusion that light frequency of Luminol ECL can be used in photoelectrochemistry of the CdS NPs was drawn, though not the optimum excitation light frequency. Compared with the traditional external light source, the photocurrent by Luminol ECL was weaker (Fig. 3 and Fig. S5 B). It was because the photons generated by Luminol ECL were less than the traditional external light source. It is worth noting that the light from Luminol ECL can be used in PEC though the photocurrent needs to be improved in future.

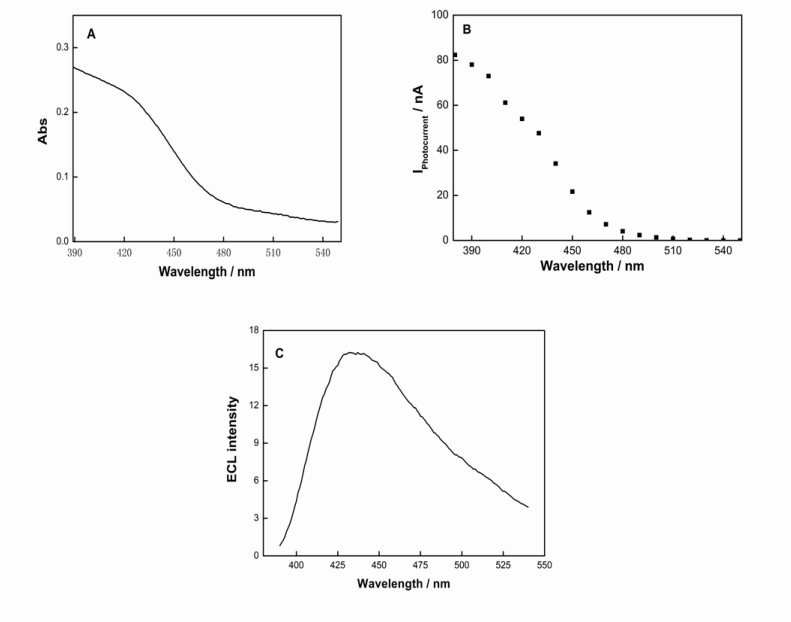

Fig. S5 (A) UV-vis adsorption spectrum of CdS NPs, (B) photocurrent spectrum of the proposed method (8×10^{-15} M of target DNA) and (C) ECL spectrum of Luminol

Principle of the readout photocurrent

Curve morphology was applied to read photocurrent. Current peak and valley on the curve occurred alternately during the procedure of determination with the proposed strategy. It is also worth highlighting that photocurrent value in this paper was the D-value of curve crest and curve hollow (eg. Fig. S6). And the time difference (ΔT) between curve crest and curve hollow previously mentioned must be compatible with ΔT in Fig. 2. The ΔT is crucial to photocurrent identification. Taking current signal of 1.0×10^{-15} M target DNA (Fig. S6 A) detections as an example, it is obvious that curve crest and curve hollow with ΔT = 60 s was observed in Fig. S6 A and no curve crest and curve hollow with ΔT = 60 s was observed in dark current (Fig. S6 B). Fig. S6 A and Fig. S6 B were magnified with the same order to identify ΔT and photocurrent. Consequently, though the photocurrent was not so strong, it can be identified from dark current.

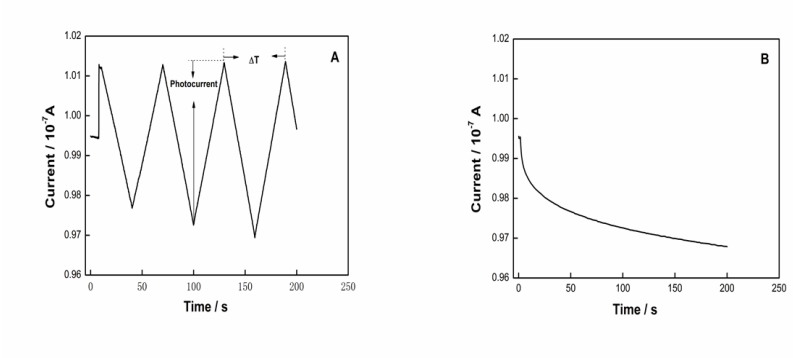

Fig. S6 Current curves of (A) 1.0×10^{-15} M target DNA, (B) dark current of 1.0×10^{-15} M target DNA

References:

1 (a) L. Jiang, X. Chen, W. Yang, J. Jin, B. Yang, L. Xu and T. Li, *Chem. J. Chin. Univ.* 2001, **22**, 1397–1399. (b) C. Ding, Q. Zhang and S. Zhang, *Biosen. Bioelectron.*, 2009, **24**, 2434–2440.

2 H. Cui, Y. Xu and Z. Zhang, *Anal. Chem.*, 2004, **76**, 4002–4010.